

# Impact of regionally increased CO<sub>2</sub> concentrations in coupled climate simulations

Tido Semmler<sup>1\*</sup>, Felix Pithan<sup>1</sup>, Thomas Jung<sup>1</sup>

<sup>1</sup> Alfred-Wegener-Institut, Helmholtz-Zentrum für Polar- und Meeresforschung  
Am Handelshafen 12  
27570 Bremerhaven

\* tido.semmler@awi.de, +49 471 4831 2287

ORCID Tido Semmler: <https://orcid.org/0000-0002-2254-4901>

ORCID Felix Pithan: <https://orcid.org/0000-0003-4382-3077>

ORCID Thomas Jung: <https://orcid.org/0000-0002-2651-1293>

## Abstract

In which direction is the influence larger: from the Arctic to the mid-latitudes or vice versa? To answer this question, CO<sub>2</sub> concentrations have been regionally increased in different latitudinal belts, namely in the Arctic, in the northern mid-latitudes, everywhere outside of the Arctic and globally, in a series of 150 year coupled model experiments with the AWI Climate Model. This method is applied to allow a decomposition of the response to increasing CO<sub>2</sub> concentrations in different regions. It turns out that CO<sub>2</sub> increase applied in the Arctic only is very efficient in heating the Arctic and that the energy largely remains in the Arctic. In the first 30 years after switching on the CO<sub>2</sub> forcing some robust atmospheric circulation changes, which are associated with the surface temperature anomalies including local cooling of up to 1°C in parts of North America, are simulated. The synoptic activity is decreased in the mid-latitudes. Further into the simulation, surface temperature and atmospheric circulation anomalies become less robust. When quadrupling the CO<sub>2</sub> concentration south of 60°N, the March Arctic sea ice volume is reduced by about two thirds in the 150 years of simulation time. When quadrupling the CO<sub>2</sub> concentration between 30 and 60°N, the March Arctic sea ice volume is reduced by around one third, the same amount as if quadrupling CO<sub>2</sub> north of 60°N. Both atmospheric and oceanic northward energy transport across 60°N are enhanced by up to 0.1 PW and 0.03 PW, respectively, and winter synoptic activity is increased over the Greenland, Norwegian, Iceland (GIN) seas. To a lesser extent the same happens when the CO<sub>2</sub> concentration between 30 and 60°N is only increased to 1.65 times the reference value in order to consider the different size of the forcing areas. The increased northward energy transport, leads to Arctic sea ice reduction, and consequently Arctic amplification is present without Arctic CO<sub>2</sub> forcing in all seasons but summer, independent of where the forcing is applied south of 60°N. South of the forcing area, both in the Arctic and northern mid-latitude forcing simulations, the warming is generally limited to less than 0.5°C. In contrast, north of the forcing area in the northern mid-latitude forcing experiments, the warming amounts to generally more than 1°C close to the surface, except for summer. This is a strong indication that the influence of warming outside of the Arctic on the Arctic is substantial, while forcing applied only in the Arctic mainly materializes in a warming Arctic, with relatively small implications for non-Arctic regions.

**Keywords:** Arctic Amplification; Arctic mid-latitude linkages; regional greenhouse gas forcing; energy transport; coupled climate model simulations

## 63 1. Introduction

64  
65 Over the last 30 years, Arctic amplification, an increase of Arctic surface temperatures twice the amount of the  
66 Northern hemisphere mean temperature increase, has been observed in the field and in climate projections  
67 (Cohen et al., 2014). This is associated with a marked sea ice decline in the Arctic which has spurred a multitude  
68 of studies investigating the impact of this strong decline on the mid-latitude weather and climate including  
69 extreme events both from observations and modelling experiments (review papers: Overland et al., 2015; Screen  
70 et al., 2018; Vavrus, 2018). In many of the modelling studies the impact of Arctic sea ice decline is mostly  
71 restricted to the stable Arctic boundary layer with only minor temperature increases higher up in the troposphere  
72 (e.g. Semmler et al., 2016a; Semmler et al., 2016b). Furthermore, the impact of shrinking sea ice in the Arctic on  
73 mid-latitudes remain subject to a large uncertainty due to a notoriously small signal-to-noise ratio in the northern  
74 mid-latitudes, a limited time period of observations, and different designs of modelling studies (Cohen et al.,  
75 2018). Since the specific region of sea ice loss plays a role in determining the large-scale circulation response  
76 (e.g. Pedersen et al., 2016), differences in the prescribed forcing in the idealized modelling studies can be  
77 important.

78  
79 Nevertheless, progress has been made. Since feedbacks between the different climate system components such  
80 as ocean, sea ice, land, and atmosphere have been recognized to be important, a number of coupled modelling  
81 studies with long integrations of 100 years or more are available now. Screen et al. (2018) give a synthesis of  
82 long coupled model experiments which reveal some consistent features as response to sea ice loss despite  
83 differences in the model set-up: hemisphere-wide atmospheric warming, intensification of Aleutian low and  
84 Siberian high, weakening of the Icelandic low, weakening and southward shift of the mid-latitude westerly winds  
85 in winter. Semmler et al. (2016b) and Petrie et al. (2015) took a different approach, running large ensembles of  
86 short integrations of only one year rather than small ensembles of long integrations, perturbing sea ice thickness  
87 in spring or early summer. Possibly due to a different start date (1st of June versus 1st of April) and different  
88 intensities of the forcing (summer ice-free conditions versus 2007/2012 conditions), results in terms of large-  
89 scale circulation response are not consistent although a southward shift of the mid-latitude westerly winds in late  
90 autumn or early winter occurs in both studies. Due to the long ocean response time, it cannot be expected that the  
91 lower latitude ocean substantially warms in these short coupled simulations. Very recently, the response to sea  
92 ice loss has been isolated from the complete greenhouse gas impact in the coordinated multi-model ensemble of  
93 CMIP5 models (Zappa et al., 2018) - the robust results being a southward shift of the jet stream and a  
94 strengthening of the Siberian High in late winter consistent with many studies prescribing idealized sea ice  
95 conditions.

96  
97 The US CLIVAR white paper by Cohen et al. (2018) has expressed a need for a common protocol for  
98 coordinated experiments to overcome the issue of different model experiment design and to further narrow down  
99 some of the uncertainties. The resulting common protocol, the Polar Amplification Model Intercomparison  
100 Project (PAMIP: Smith et al., 2018) has been endorsed by CMIP6. Experiments within PAMIP include applying  
101 Arctic sea ice anomalies with and without SST anomalies in uncoupled and coupled mode in short 1-year and  
102 long 100-year simulations. While it was relatively straightforward to agree on a protocol for the uncoupled  
103 experiments, prescribing sea ice and SST, the design of the coupled experiments has been much more  
104 controversial since the sea ice is an interactive component of the coupled model system and thus cannot be  
105 prescribed. Therefore, the sea ice relaxation approach is only suggested in the PAMIP protocol for the coupled  
106 experiments but is not the only choice allowed to achieve a sea ice reduction (Smith et al., 2018). This motivated  
107 us to experiment with an alternative approach.

108  
109 It is acknowledged that Arctic amplification is influenced not only by local processes (e.g. Pithan and Mauritsen,  
110 2014) but also by the mid- and lower latitudes such as mid-latitude SST (e.g. Luo et al., 2018) and circulation  
111 changes (e.g. Gong et al., 2017) leading to more frequent moisture intrusions into the Arctic (e.g. Woods and  
112 Caballero, 2016). Many recent studies have focused on Arctic-to-mid-latitude influences. Here we ask what  
113 direction exhibits the stronger coupling: from the Arctic to the Northern mid-latitudes or vice versa. To answer  
114 this question, it is not sufficient to alter sea ice conditions as this can only be done in the polar regions, not in the  
115 mid-latitudes. Furthermore, the ocean should be included as it can play an important role in the energy transport.  
116 Therefore, long integrations are needed. To keep the computational burden manageable, we opted to run the  
117 simulations in a relatively coarse resolution. Our idea is to increase CO<sub>2</sub> forcing regionally in the Arctic and in  
118 this way trigger Arctic amplification. Results can be contrasted against simulations with CO<sub>2</sub> forcing outside of  
119 the Arctic. This approach has very recently been applied by Stuecker et al. (2018) using the Community Earth  
120 System Model CESM 1.2. We complement their study using another CMIP6 model (AWI-CM 1.1) and  
121 additionally investigate the large-scale circulation response. Furthermore, we ran the coupled system for 150  
122 years rather than 60 years which allows us to compare the transient response in the first decades after regionally  
123 increasing CO<sub>2</sub> to the response after the ocean had time to react.

125 In section 2 the experiment set up is described. Section 3 explains our results; discussion and conclusions follow  
126 in section 4.

127

## 128 **2. Experiment setup**

129

130 As stated in the introduction, there is a lot of discussion about how to study the influence of declining sea ice on  
131 mid-latitudes in coupled simulations. The most common methods are applying a ghost longwave radiation  
132 forcing over the sea ice covered area, a change of the sea ice albedo, and a relaxation of the sea ice concentration  
133 to some desired distribution such as projected end-of-the-century conditions (e.g. Screen et al., 2018). Here, we  
134 experiment with an approach to perturbing coupled models very recently introduced by Stuecker et al. (2018).  
135 The idea is to increase the CO<sub>2</sub> concentration in some area of interest. In our study, we quadruple CO<sub>2</sub> north of  
136 60°N (experiment called 60N hereafter), north of 70°N (70N), north of the simulated ice edge on the 1st of  
137 January each year (SICE), in a latitude band from 30 to 60°N (30-60N), south of 60°N (60Ns) or globally (glob)  
138 - for an overview see Fig. 1 showing Arctic sea ice volume from the different experiments. The experiment 30°N  
139 to 60°N is additionally run with 1.65\*CO<sub>2</sub> (30-60N\_1.65) to account for the different size of the forcing area in  
140 order to make the 30-60N\_1.65 and the 60N experiments directly comparable. Indeed the 30-60N\_1.65 and the  
141 60N experiment have the same globally averaged radiative forcing within the error estimates. This has been  
142 checked with a Gregory diagnosis (Gregory et al., 2004): 0.45 +/- 0.09 W/m<sup>2</sup> for the 30-60N\_1.65 experiment  
143 and 0.48 +/- 0.09 W/m<sup>2</sup> for the 60N experiment.

144

145 The simulations are set up in the spirit of the HighResMIP protocol (Haarsma et al., 2016), i.e. the control  
146 simulation (ctl) is run for a total of 200 years with the first 50 years regarded as spin-up. After the spin-up  
147 period, the described sensitivity experiments are run for 150 years which are then compared to the corresponding  
148 years of the ctl simulation. All simulations are run with the Alfred Wegener Institute Climate Model version 1.1  
149 (AWI-CM 1.1). AWI-CM has been described in Sidorenko et al. (2016), Rackow et al. (2018), and Rackow et al.  
150 (2019). The model was run in its low resolution CMIP6 set-up (LR). The atmosphere model is ECHAM6.3 in  
151 T63L47 resolution corresponding to about 200 km horizontal resolution and 47 unequally spaced vertical levels  
152 up to 80 km. The ocean model is the Finite Element Sea ice Ocean Model FESOM 1.4 which runs on an  
153 unstructured mesh with an average horizontal resolution of around 70 km and local refinement in the tropics, the  
154 northern North Atlantic, the Arctic, and the coasts. In the vertical there are 46 unequally spaced z-levels.

155

156 The regional CO<sub>2</sub> method has certain advantages over previously used methods, i.e. the model itself is not  
157 altered through the introduction of extra fluxes or relaxation terms which would make the model non-energy-and  
158 non-mass-conserving. Unlike the albedo reduction method, the forcing is applied all year rather than only in  
159 summer. Furthermore, it is possible to perform comparative experiments with forcing in other latitudes.  
160 However, also with this method of regionally increasing the CO<sub>2</sub> concentration the baroclinicity is altered by  
161 definition.

162

163 Fig. 1 shows that the regional CO<sub>2</sub> method works to reduce Arctic sea ice quite fast within about one decade. In  
164 addition to the rapid response of the sea ice in all sensitivity experiments, a slow long-term drift possibly due to  
165 oceanic processes occurs for the global and nearly global forcing experiments (glob and 60Ns). Even without  
166 any Arctic forcing in the 60Ns experiment, the amount of Arctic sea ice declines markedly due to energy  
167 transport from the low to the high latitudes. If forcing is applied only in the northern mid-latitudes (30-60N\_1.65  
168 and 30-60N), Arctic sea ice is also shrinking, especially in the 30-60N experiment where the reduction is  
169 comparable to the 60N experiment. The experiments allow study of the transient phase of rapid sea ice loss and  
170 the stabilization phase. Results regarding atmospheric temperature response, large-scale circulation, synoptic  
171 activity, and energy transport are described in the next section.

172

## 173 **3. Results**

174

### 175 **3.1. Atmospheric temperature response**

176

177 The zonally averaged vertical temperature profile anomalies for the 60N simulation for the first 30 years after  
178 regionally quadrupling CO<sub>2</sub> are shown in Fig. 2. The profiles indicate mainly near-surface warming, except for  
179 summer where the atmospheric boundary layer is less stable and more mixing takes place. In winter, noticeable  
180 warming of more than 0.5°C is restricted to layers below 500 hPa. Laterally such warming spreads to around  
181 48°N. In the following 120 years, the picture does not look very different (Fig. 3), although the warming spreads  
182 out a little bit more laterally due to the gradual heat uptake of the ocean. Warming of more than 0.5°C occurs up  
183 to 44°N in these 120 years. In addition, slight warming of 0.2 to 0.5°C occurs almost everywhere in the  
184 troposphere north of 20°N which is not the case for the first 30 years. Due to the weaker forcing in 70N and  
185 SICE simulations, warming areas are vertically more restricted in those simulations (not shown). The vertical

186 restriction of the warming is in line with previous studies of the effects of declining sea ice (e.g. Screen et al.,  
187 2013; Semmler et al., 2016a).

188  
189 In the simulations we see some stratospheric cooling (Figs. 2 and 3) which is opposite from what we have  
190 observed in recent decades. This cooling becomes even stronger in the last 120 years compared to the first 30  
191 years of the simulation. Previous simulations have shown strong intrinsic variability and inter-model differences  
192 in the stratospheric response to sea ice reduction in both uncoupled and coupled simulations (Screen et al., 2013;  
193 Screen et al., 2018) which could suggest that also the stratospheric warming that we have observed over the last  
194 three decades might not be due to sea ice decline but simply an expression of intrinsic variability or lower  
195 latitude impacts. Indeed, Seviour (2017) and Garfinkel et al. (2017) confirm by evaluating large ensembles of  
196 coupled climate model simulations that vortex trends of similar magnitude to those observed can be generated by  
197 internal variability. Due to the stratospheric cooling our simulated large-scale circulation response to AA might  
198 be different compared to studies with stratospheric winter warming. It should be noted that it is not clear in  
199 which direction the stratospheric polar vortex is headed under global warming scenarios (Ayarzagüena et al.,  
200 2018).

201  
202 Figs. 4 and 5 show the zonally averaged vertical temperature profile anomalies for the 30-60N and 30-60N\_1.65  
203 experiments. To account for the different strength of the globally averaged radiative forcing in the 30-60N  
204 simulation compared to 60N and 30-60N\_1.65 simulations, the response in the 30-60N simulation is scaled by  
205 the different forcing area between 60N and 30-60N simulations. As expected, the warming spreads out higher up  
206 into the troposphere in 30-60N and 30-60N\_1.65 experiments compared to 60N experiment, generally up to 200  
207 to 300 hPa rather than 500 hPa. Laterally, the warming mainly spreads out to the Arctic in the 30-60N and 30-  
208 60N\_1.65 experiments and amounts to more than 1°C in large areas in all seasons but summer. In contrast, south  
209 of the forcing area, i.e. south of 30°N the warming only exceeds 0.5°C in a 2-7 degree latitude belt depending on  
210 the season and on the experiment. It is reassuring that the stronger globally averaged radiative forcing in the 30-  
211 60N simulation compared to the 30-60N\_1.65 simulation does not qualitatively change the vertical profile of the  
212 zonally averaged temperature response. However, even the scaled warming appears to be slightly larger in the  
213 30-60N simulation compared to the 30-60N\_1.65 simulation. In the 60Ns experiment (Fig. 6), a largely  
214 homogeneous warming corresponding to a scaled value of 0.2 to 0.5°C is simulated. Only in the subtropical  
215 troposphere as well as close to the surface in the Arctic in winter, spring, and autumn larger temperature  
216 increases are simulated which resembles a typical response pattern to global CO<sub>2</sub> forcing.

217  
218 Very little of the extra energy due to the regional CO<sub>2</sub> forcing spreads towards the equator; the bulk of the extra  
219 energy spreads towards the pole leading to Arctic Amplification associated with Arctic sea ice melt in all seasons  
220 but summer. The typical bottom heavy Arctic Amplification signature can be seen both in the northern mid-  
221 latitude forcing experiments (Figs. 4 and 5) and in the extra-Arctic forcing experiment 60Ns (Fig. 6). In section  
222 3.3 the meridional atmospheric and oceanic energy transport is analyzed to understand these responses.

### 223 224 **3.2 Near-surface temperature response in the Arctic forcing experiments**

225  
226 After quadrupling CO<sub>2</sub> in the Arctic we already see strong surface warming in this region in the first 30 years -  
227 as expected (Fig. 7). In this Figure we only show changes in the 60N experiment but the changes are consistent  
228 in the 3 experiments 60N, 70N, and SICE and are robust. Especially robust is the Barents Sea warming of more  
229 than 7°C compared to the 1950 control experiment. This warming is caused by the maximum of sea ice loss in  
230 this area (not shown). In cases of northerly flows we would expect mid-latitude warming and less temperature  
231 variability due to the advection of less cold air (Semmler et al., 2012; Ayarzagüena and Screen, 2016) which we  
232 indeed see in many areas, especially over central Eurasia and the North Pacific (only mean signal shown, not  
233 variability). However, we see robust winter cooling by up to around 1°C over Central North America as well as  
234 by more than 0.2°C over eastern Asia and off its coast in the transient phase of the first 30 years after  
235 quadrupling CO<sub>2</sub> (Fig. 7a). In addition, no warming or a slight cooling of up to around 0.2°C is simulated over  
236 the British Isles, parts of the North Atlantic and western Scandinavia, for western Scandinavia only for 70N and  
237 SICE simulations (not shown). These temperature anomalies are consistent with the geopotential height  
238 anomalies in 500 hPa (Fig. 8, up to around 50 m) indicating a barotropic response. The forcing excites a wave  
239 train with PNA (Pacific North America pattern) and EA (East Atlantic pattern) like anomalies. We also see a  
240 southward deflection of the jet stream in the eastern North Atlantic regions, redirecting the jet towards the  
241 Mediterranean Sea in the first 30 years after regionally quadrupling CO<sub>2</sub> (Fig. 9).

242  
243 In the second and third 30 year periods (Fig. 7b,c) some of the regional cold anomalies still persist (no warming  
244 over North Atlantic and slight cooling off the northeastern coast of Asia) but the large cold anomaly of up to  
245 around 1°C over Central North America is replaced by a warm anomaly. Especially in the third 30 year period  
246 regional cold anomalies occur over other areas (Fig. 7c) but are not consistent across 60N, 70N, and SICE  
247 simulations and therefore not robust (not shown). Regional deviations from the zonal mean response are smaller

248 in the second and third 30 year periods compared to the first 30 year period. In the last 60 years (Fig. 7d,e), apart  
249 from the strong warming over the Arctic that decreases with decreasing latitude within the northern mid-  
250 latitudes, a slight but rather homogeneous warming of around 0.2°C prevails. Therefore, regional deviations  
251 from the zonal mean response in the last two 30 year periods are smallest within the five 30 year periods.  
252 Similarly as for the 2 m temperature, for 500 hPa geopotential height and 300 hPa zonal wind regional anomalies  
253 become less robust over time (not shown). A reason for the weakening of the regional deviations from the zonal  
254 mean response over the simulation time, both in magnitude and robustness, could be that the ocean gradually  
255 warms; first adjacent to the Arctic forcing area and then the warming spreads out further, especially in the 60N  
256 simulation. The slow adjustment of the ocean spreads out the initial temperature gradient weakening between  
257 Arctic and northern mid-latitudes to the south, making it again slightly stronger at the boundary of the forcing  
258 area. However, the meridional energy transport and the synoptic activity considered in the following two  
259 subsections do not show any trend towards a weakening response with simulation time.

260  
261 Except for the temperature anomalies in the Arctic itself, temperature and circulation anomalies are rather small  
262 compared to the large intrinsic variability of the system, even in the first 30 years after quadrupling CO<sub>2</sub> in the  
263 Arctic. Anomalies generally do not exceed 1°C for the 2 m temperature, 50 m for Z500, and 5 m/s for the zonal  
264 wind in 300 hPa. One exception is the cold 2 m temperature anomaly over parts of North America related to the  
265 PNA-like anomaly in the first 30 years. Generally, our study prescribing greenhouse gas forcing above and  
266 around the sea ice area confirms the weak response to Arctic sea ice anomalies that was found in previous  
267 studies. .

### 268 269 **3.3 Meridional energy transport**

270  
271 An analysis of the atmospheric meridional energy transport (Fig. 10a,c) reveals a decrease of the northward  
272 energy transport between around 35°N and 80°N in the Arctic forcing simulations 60N, 70N, and SICE  
273 compared to the control run. The decrease is most pronounced in the 60N simulation (up to 0.13 PW). In other  
274 latitude belts differences are very small. This holds for both the first 30 years and also the following 120 years.  
275 The 30-60N and 30-60N\_1.65 simulations show increased northward energy transport north of around 50°N (up  
276 to 0.08 PW in 30-60N simulation in the first 30 years) and a decreased northward energy transport south of  
277 around 50°N (up to 0.2 PW in 30-60N simulation in the last 120 years) extending southward to about 10 to 50°S  
278 depending on the considered time period and on the intensity of the forcing (30-60N\_1.65 compared to 30-60N).  
279 It is reassuring that qualitatively 30-60N and 30-60N\_1.65 simulations agree, i.e. scaling of the response with the  
280 magnitude of the forcing is justified.

281  
282 The 60Ns and glob simulations show large anomalies with respect to the control simulation across all latitudes  
283 which are due to the nearly global or global CO<sub>2</sub> forcing. The anomalies generally work towards increased  
284 southward atmospheric energy transports in the Southern Hemisphere and towards increased atmospheric  
285 northward energy transports in the Northern Hemisphere, making the meridional energy transport towards the  
286 poles stronger almost everywhere. The response appears to be roughly additive, i.e. when adding the anomalies  
287 of the 60N and the 60Ns simulations (dashed orange lines in Fig. 10a,c), the result is similar to the anomalies of  
288 the glob simulation (solid orange lines in Fig. 10a,c); differences are smaller than 0.03 PW and are further  
289 decreasing over simulation time (compare Fig. 10a with Fig. 10c). This gives credibility to the regional forcing  
290 approach and is in agreement with Stuecker et al. (2018). However, the small differences between the sum of  
291 60N and 60Ns simulations and the glob simulation are in the same direction across all latitudes north of 40°S  
292 and may therefore point to an important difference. The sum of 60N and 60Ns simulations shows a slightly  
293 stronger atmospheric northward energy transport across all latitudes north of 40°S than the glob simulation  
294 (compare dashed orange line in Fig. 10a with solid orange line). This can be attributed to the increased  
295 northward atmospheric energy transport in the 60Ns simulation (brown line in Fig. 10a) compared to the glob  
296 simulation (solid orange line in Fig. 10a) which arises over all latitudes north of around 40°S. In contrast, when  
297 comparing the 60N simulation to the control simulation (black curve in Fig. 10a) - which differs in the same way  
298 as the glob simulation from the 60Ns simulation, namely by 4\*CO<sub>2</sub> instead of 1\*CO<sub>2</sub> in the Arctic -, anomalies  
299 in the northward atmospheric energy transport remain close to 0 south of around 30°N.

300  
301 In the ocean (Fig. 10b,d) the situation is not as clear cut. Changes beyond the northern mid-latitudes occur also  
302 in the Arctic forcing simulations, for the larger forcing area (60N) already in the first 30 and also in the  
303 following 120 years and for the weaker forcing areas (70N and SICE) only in the following 120 years.  
304 Furthermore, no systematic difference can be seen between the sum of 60N and 60Ns simulations on one hand  
305 and the glob simulation on the other hand, at least not in the first 30 years. In the following 120 years there is a  
306 slight tendency towards stronger northward energy transport in the sum of 60N and 60Ns simulations compared  
307 to the glob simulation. Anomalies in the global and nearly global forcing experiments glob and 60Ns generally  
308 work towards a weaker poleward oceanic energy transport which is in contrast to the atmospheric transport.  
309 While in the ocean anomalies clearly grow over time for all simulations - around 20°S by as much as 0.25 PW in

310 the global and nearly global forcing experiments when comparing the last 120 years to the first 30 years - in the  
311 atmosphere they grow only slightly by less than 0.05 PW or they remain constant.

312

### 313 **3.4 Synoptic activity**

314

315 The reduced atmospheric northward energy transport in the Arctic forcing experiments is also reflected by a  
316 slightly reduced synoptic activity in the northern mid-latitudes (Fig. 11a for the 60N experiment in winter, also  
317 true for 70N and SICE experiments and for the other seasons) due to reduced meridional temperature gradients  
318 in these experiments which can cause less energy exchange. An exception is the area over the Greenland,  
319 Norwegian, Iceland (GIN) Seas in winter (Fig. 11a) and the Arctic north of 80°N in summer (not shown) where  
320 the synoptic activity increases by up to 2-3 m - which is very little compared to the variability in these areas.

321

322 Similarly, the increased atmospheric northward energy transport north of 50°N in the mid-latitude forcing  
323 experiments is generally reflected by an increased synoptic activity in these latitudes, especially over the GIN  
324 seas, and the decreased energy transport south of 50°N by a decreased synoptic activity (Fig. 11b and 11c for  
325 winter, also true for the other seasons).

326

327 In the 60Ns and glob experiments there are areas of strengthened and weakened synoptic activity (not shown).  
328 Especially in the Southern Hemisphere the poleward shift of intense synoptic activity typical for greenhouse gas  
329 increase experiments (e.g. Tamarin and Kaspi, 2017) becomes obvious. In the Northern Hemisphere no poleward  
330 shift occurs. Instead, an intensification of synoptic activity along the jet stream path over the North Pacific and  
331 an eastward extension over the North Atlantic into Europe is simulated. In summary, in the 30-60N, 30-  
332 60N\_1.65, 60Ns and glob experiments synoptic activity is redistributed while in the Arctic forcing experiments it  
333 is reduced with the reduction being confined to the area of meridional temperature gradient reduction.

334

335 The weak linkage between the mid-latitudes and the Arctic in the Arctic forcing simulations is reflected by a  
336 large decrease of Arctic sea ice volume (Fig. 1 black and grey lines, around 12,000 km<sup>3</sup> in 60N compared to  
337 control) - an indication that the extra energy stays in the Arctic and causes melting of the sea ice. The same  
338 Arctic sea ice volume decrease is simulated when 4\*CO<sub>2</sub> is applied in the northern mid-latitudes 30-60°N (Fig.  
339 1, purple line). Obviously, when the magnitude of the global radiative forcing is considered to make the northern  
340 mid-latitude forcing simulation comparable to the Arctic forcing simulation, the Arctic sea ice volume decrease  
341 is weaker (Fig. 1, green line).

342

### 343 **4. Discussion and conclusions**

344

345 In this study, a novel approach is used to explore the impact of Arctic climate change on mid-latitudes and vice  
346 versa in a coupled climate model. In this approach, which recently has been also employed by Stuecker et al.  
347 (2018), atmospheric CO<sub>2</sub> concentrations are quadrupled in certain regions, while keeping other regions  
348 unchanged. An important result of this study, which is consistent with previous work, is that the Arctic generally  
349 shows a relatively limited influence on extra-Arctic regions, while CO<sub>2</sub> changes in the extra-Arctic region lead  
350 to substantial changes in the Arctic. The energy added in the regional Arctic forcing experiments stays in the  
351 Arctic causing efficient reduction of the Arctic sea ice; the synoptic activity is reduced, weakening the link  
352 between Arctic and mid-latitudes. Nevertheless, there are some important insights to be gained from the regional  
353 Arctic forcing experiments which are described in the following before turning to the extra-Arctic forcing.

354

355 When Arctic sea ice is reduced because of the CO<sub>2</sub> forcing, the vertical temperature profile in the atmosphere  
356 changes in the Arctic. In the Arctic troposphere, the changes are consistent with those found in previous studies  
357 reducing Arctic sea ice, i.e. most of the warming takes place close to the surface. However, in the Arctic  
358 stratosphere cooling is simulated. Our simulations, thus, suggest that there is a stronger stratospheric polar vortex  
359 in late winter in contrast to a weaker one like some previous studies investigating the response to reduced Arctic  
360 sea ice reported (e.g. Jaiser et al., 2013; Kim et al., 2014) - although the stratospheric response is sensitive to the  
361 location of Arctic sea ice loss (e.g. Sun et al., 2015). The strengthened stratospheric polar vortex in our Arctic  
362 forcing experiments needs to be taken into consideration when interpreting the results presented here. Even  
363 though it has been observed that the intensity of the stratospheric polar vortex has decreased in recent decades  
364 (e.g. Kretschmer et al., 2018), it is not clear if this is due to Arctic sea ice decline or due to other factors. Also  
365 unclear is how the stratospheric polar vortex will develop in a warming climate (Ayarzagüena et al., 2018).

366

367 In our study, we use a different model than Stuecker et al. (2018) (AWI-CM 1.1 instead of CESM2) and consider  
368 different regions (more focus on the Arctic region with three different set-ups as well as the northern mid-  
369 latitudes with two different set-ups while leaving the Southern Hemisphere untouched). Furthermore, we also  
370 consider longer time scales, which gives us an insight into the transient versus the quasi-equilibrium response;  
371 and additional analyses are carried out that address large-scale circulation changes including synoptic activity.

372  
373 An important result is that only in the adjustment phase in the first 30 years after adding the perturbation, there  
374 are robust regional near-surface temperature and large-scale circulation changes such as surface cooling of more  
375 than 1°C over parts of North America and up to around 0.2°C over eastern Asia in winter. The pattern of  
376 strongest warming over the Barents-Kara Seas and the East Siberian and-Chukchi Sea areas along with cold  
377 anomalies over North America and over eastern Asia are reminiscent of the observed temperature trend pattern  
378 of the last two decades (e.g. Kug et al., 2015) although in our simulations the East Siberian and-Chukchi Sea  
379 warming is extended into the Beaufort Sea, and the cold anomaly is restricted to the very eastern parts of Asia.  
380 The latter pattern could be caused by the fact that we do not have a weakening but a strengthening of the  
381 stratospheric polar vortex. Therefore, weak stratospheric vortex events are less likely in our Arctic forcing  
382 experiments. However, more weak stratospheric vortex events have occurred in the recent two decades. Through  
383 downward propagation this can cause northern Eurasia cold events. Indeed this had led to a cooling trend even in  
384 the average in some Northern Eurasian areas (e.g. Kretschmer et al., 2018). The strengthening of the  
385 stratospheric polar vortex along with the advection of less cold air in cases of northerly flow could lead to the  
386 relatively strong warming trend over northern Eurasia in our Arctic forcing experiments.

387  
388 After the first 30 years, the magnitude of the anomalies decreases. This is an important result given that the most  
389 rapid Arctic changes were observed in the last 30 years. Because of this similarity between observations and  
390 model simulations, one might speculate if once a hiatus in Arctic amplification occurs for example due to natural  
391 variability, the expected circulation and temperature anomalies would decrease in intensity or even disappear.  
392 However, our experiments are highly idealized and our experiments consider a sudden rather than transient  
393 forcing which then leads to transient changes.

394  
395 A plausible explanation of the behavior in the simulations could be that the initial warming occurring in the  
396 Arctic due to the regional CO<sub>2</sub> forcing spreads out slowly into lower latitudes due to the long ocean adjustment  
397 time scale. In this respect our results agree with the coupled Arctic sea ice reduction experiments described in  
398 Screen et al. (2018). Therefore, the initial differential heating is not restricted to the Arctic anymore. The initial  
399 marked meridional temperature gradient reduction around 60°N is getting spread out towards lower latitudes.  
400 However, the meridional energy transport and the synoptic activity response do not show any trend towards a  
401 weaker response with simulation time.

402  
403 It has also been discussed if a weaker meridional temperature gradient may cause more extreme events due to a  
404 weakened jet stream and amplified and slower moving planetary waves. However, given the shallowness of the  
405 Arctic temperature increase and the strong natural variability it is difficult to get a robust response (Vavrus,  
406 2018). When we look at the variability on time scales beyond the synoptic scale in our three Arctic forcing  
407 simulations we see a robust, up to around 0.5°C higher 2-m winter temperature variability over Siberia in the  
408 first 30 years. In other regions there is no consistent pattern. Averaged over the northern mid-latitudes there is  
409 not much change. After the first 30 years there is a decrease in 2 m winter temperature variability in most  
410 northern mid-latitude areas.

411  
412 While there are some consistent but weak mid-latitude features in the transient response to the regional Arctic  
413 forcing, the influence of extra-Arctic forcing on the Arctic is clearly more important. Efficient Arctic sea ice  
414 reduction can occur in absence of Arctic CO<sub>2</sub> forcing by quadrupling CO<sub>2</sub> only south of 60°N (extra-Arctic  
415 forcing) or in the northern mid-latitudes between 30 and 60°N. While the temperature close to the surface  
416 strongly increases north of the forcing area 30-60°N, this does not happen south of the forcing area. This is also  
417 true when the forcing in 30-60°N is reduced to 1.65\*CO<sub>2</sub> in order to consider the larger forcing area compared  
418 to the area of north of 60°N. Due to an increased northward atmospheric energy transport and increased high-  
419 latitude synoptic activity in the extra-Arctic and northern mid-latitude forcing simulations, Arctic sea ice  
420 reduction is triggered, and consequently Arctic Amplification occurs, despite the lack of Arctic CO<sub>2</sub> forcing. In  
421 the extra-Arctic and global forcing experiments an increased high-latitude northward oceanic energy transport of  
422 up to 0.1 PW occurs. This could also contribute to Arctic sea ice decline and Arctic Amplification; the slow  
423 component of Arctic sea ice decline in Fig. 1 in these simulations supports this notion. In the Arctic forcing  
424 experiments decreased northward atmospheric energy transport compared to the control simulation is only  
425 present in the northern high- and mid-latitudes. Therefore, the Arctic forcing only impacts the mid-latitudes in  
426 the atmosphere. However, in the ocean the Arctic forcing does play a role also for the low latitude northward  
427 energy transport which is decreased compared to the control simulation at least after the initial 30 years by up to  
428 0.12 PW.

429  
430 While the atmospheric energy transport is generally larger in magnitude than the oceanic energy transport by a  
431 factor of around 3 in northern high-latitudes in all experiments, the anomalies between sensitivity experiments  
432 on one hand and the control experiment on the other hand are of comparable magnitude (see Fig. 10). This  
433 indicates that the ocean plays an important role in redistributing the energy in the sensitivity experiments. For the

434 northern mid-latitude forcing experiments, the ocean even plays a larger role in the redistribution of the extra  
435 energy compared to the atmosphere. Anomalies in low latitude northward energy transport amount to up to -0.35  
436 PW in the ocean and only up to -0.2 PW in the atmosphere.

437  
438 In the first 15 years of the 60Ns simulation around half of the Arctic sea ice volume is gone due to the CO<sub>2</sub>  
439 forcing south of 60°N (Fig. 1). In the remaining 135 years of the simulation another sixth of the original Arctic  
440 sea ice volume disappears bringing the total reduction to two thirds. The fast adjustment in the first 15 years  
441 versus the slower adjustment in the remaining simulation time indicates that the atmospheric contribution to the  
442 sea ice melt decreases over time.

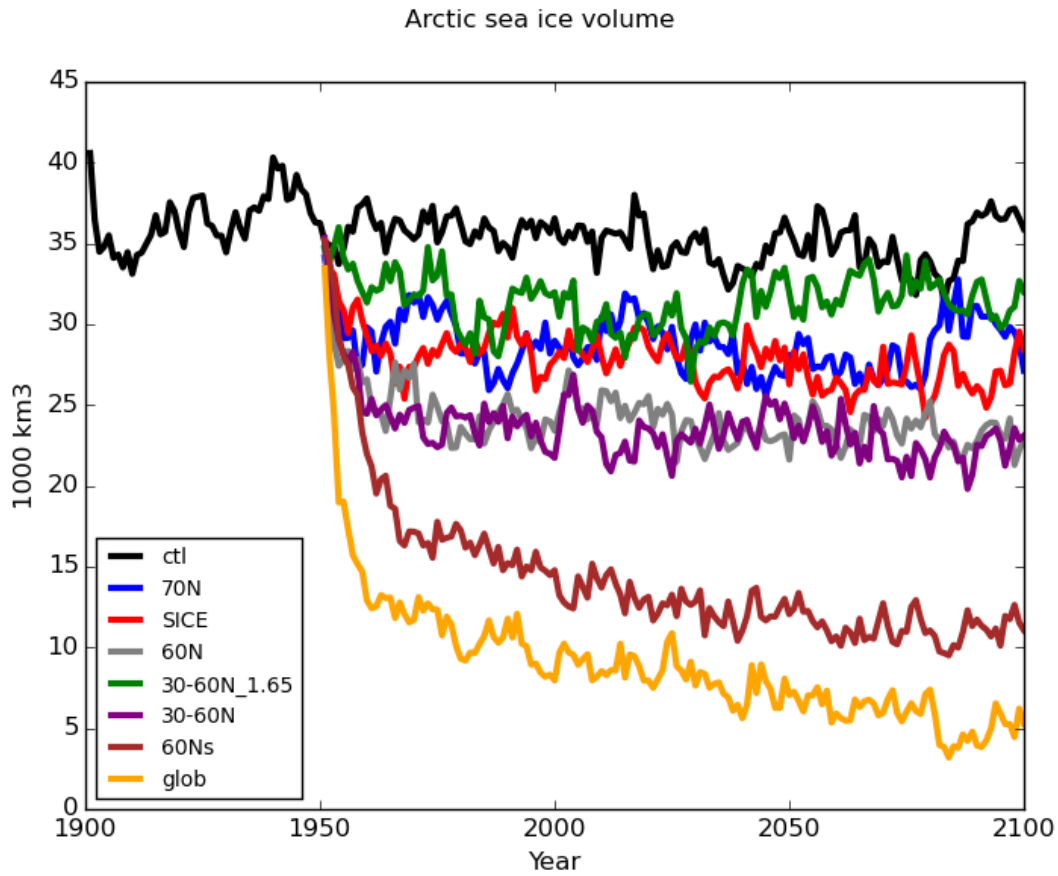
443  
444 We propose that the method of regionally increased CO<sub>2</sub> concentrations should be used in a set of coordinated  
445 experiments with as many different climate models as possible. The PAMIP community could decide to take  
446 such experiments onboard as additional experiments since it has been shown by both Stuecker et al. (2018) and  
447 in this study that the method works to decompose the regional impacts of CO<sub>2</sub> concentrations. However, there  
448 are important differences in the results between the two studies. In our study the meridional oceanic and  
449 atmospheric energy transport plays a major role for Arctic amplification while Stuecker et al. (2018) point to the  
450 local processes as a major source of Arctic amplification. In our study the response in the meridional  
451 atmospheric energy transport to the regional forcing is additive in the polar regions while in the low latitudes an  
452 increased northward energy transport is simulated for the sum of extra-Arctic forcing and Arctic forcing  
453 compared to the global forcing.

454  
455 It is not clear if the differences between the two studies are due to the different model formulations or due to the  
456 different experiment set-up (in the case of Stuecker et al., 2018, the forcing is symmetric between the two  
457 hemispheres; in our case the set-up is asymmetric). Therefore the call for coordinated experiments. Causes and  
458 impacts of Arctic amplification could be studied in an idealized and consistent way, and the robustness of the  
459 results could be checked by comparing multiple climate models.

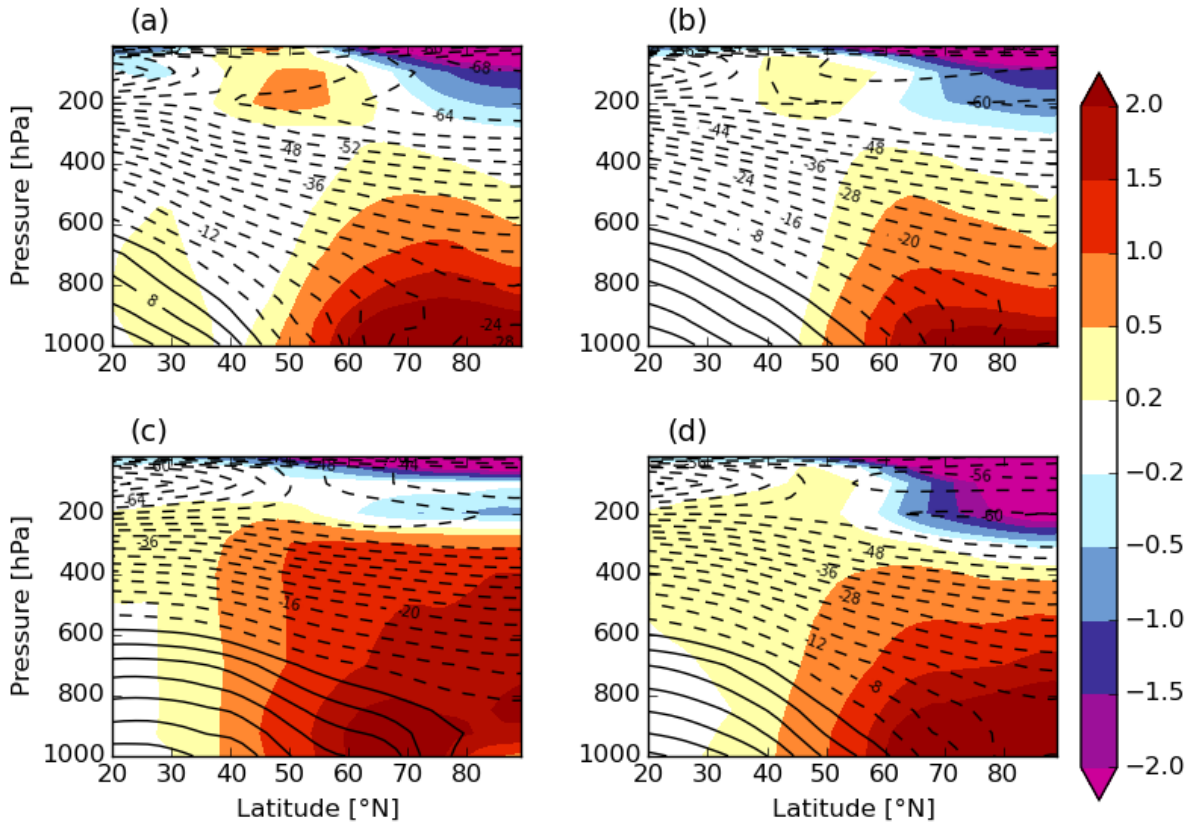
#### 460 **Acknowledgements**

461  
462 We are grateful to the DKRZ (German computing center) for providing us with computing time. This work has  
463 been carried out within the project APPLICATE which has received funding from the European Union's Horizon  
464 2020 research and innovation programme under grant agreement No. 727862. We thank Claudia Hinrichs for  
465 critical reading of our manuscript and her constructive comments. Furthermore we thank the anonymous  
466 reviewer for constructive comments and suggestions.

#### 467 **Figures**

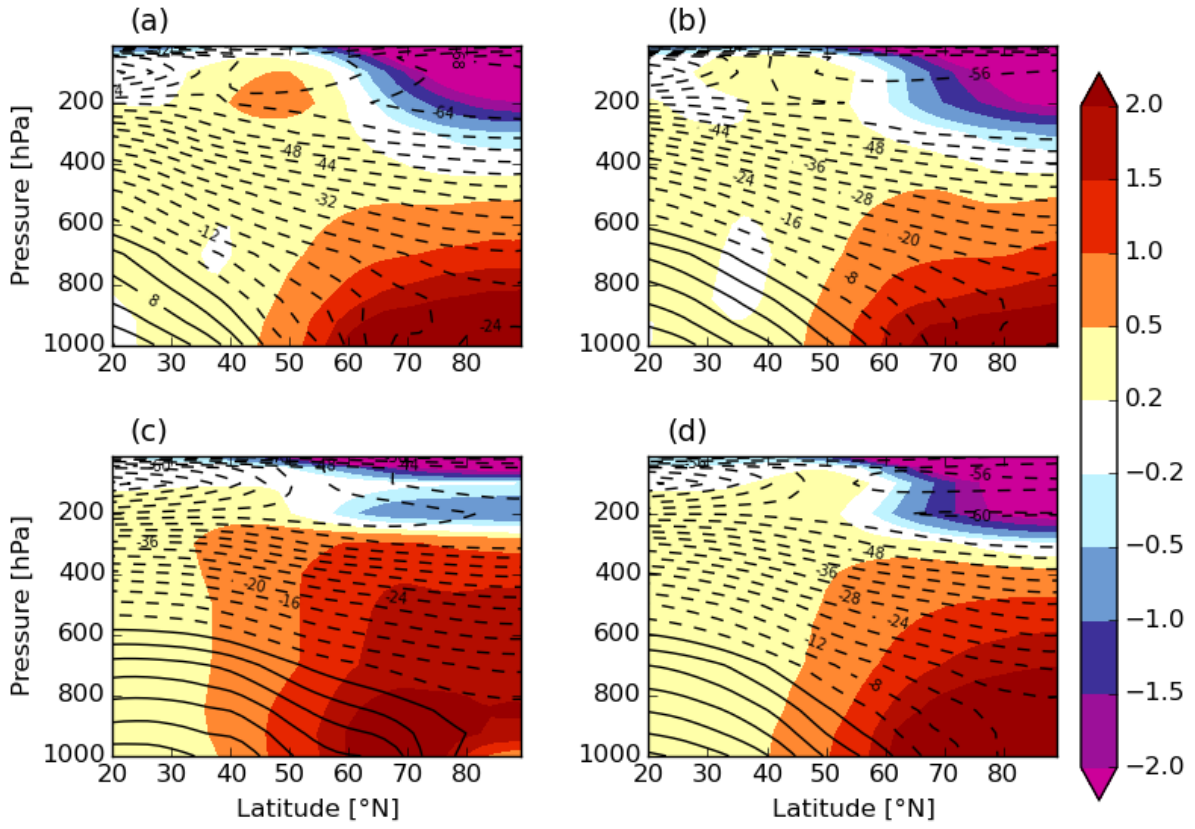


470  
 471  
 472 Fig. 1: Time series of Arctic sea ice volume in March for the control integration with 1950 CO<sub>2</sub> forcing (ctl) and  
 473 different sensitivity experiments, in which CO<sub>2</sub> is instantaneously increased in 1950: quadrupled north of 70°N  
 474 (70N), quadrupled north of the sea ice edge on the 1st of January each year (SICE), quadrupled north of 60°N  
 475 (60N), multiplied by 1.65 between 30 and 60°N (30-60N\_1.65), quadrupled between 30 and 60°N (30-60N),  
 476 quadrupled south of 60°N (60Ns), and quadrupled globally (glob).  
 477



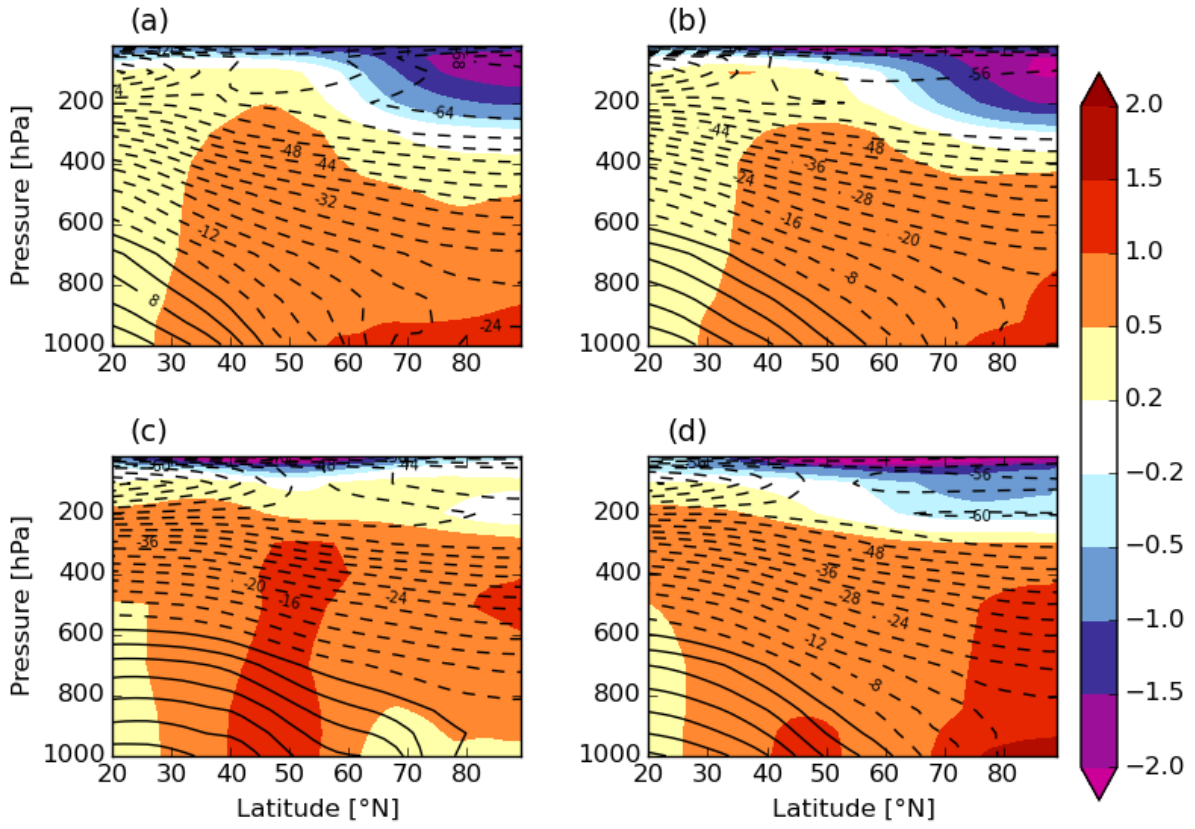
478  
 479  
 480  
 481  
 482  
 483  
 484

Fig. 2: Response in zonally averaged temperature averaged over the first 30 years after quadrupling CO2 north of 60°N (in the Arctic) in (a) winter, (b) spring, (c) summer, and (d) autumn. Solid and dashed lines indicate above- and sub-zero temperatures in the 1950 control simulation, shaded contours indicate anomalies in the sensitivity simulation.



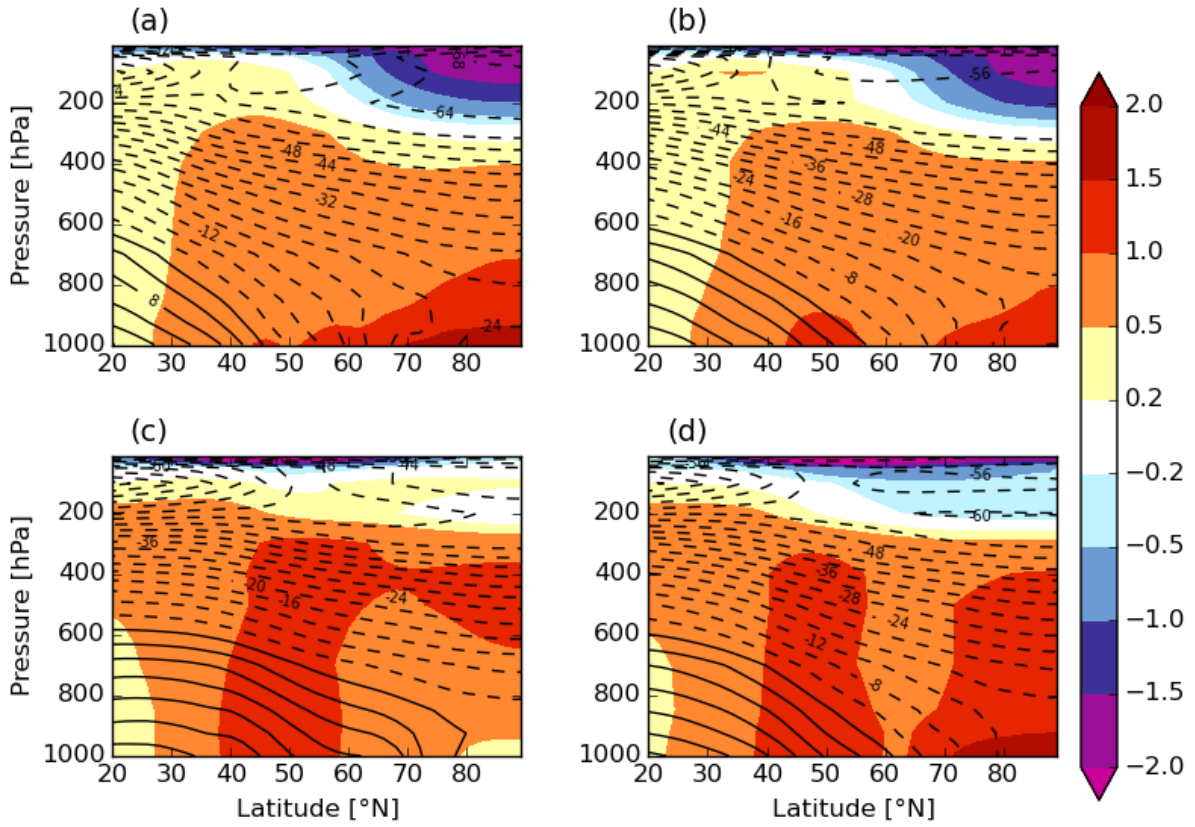
485  
 486  
 487  
 488  
 489  
 490

Fig. 3: As in Fig. 2 but averaged over the last 120 years.



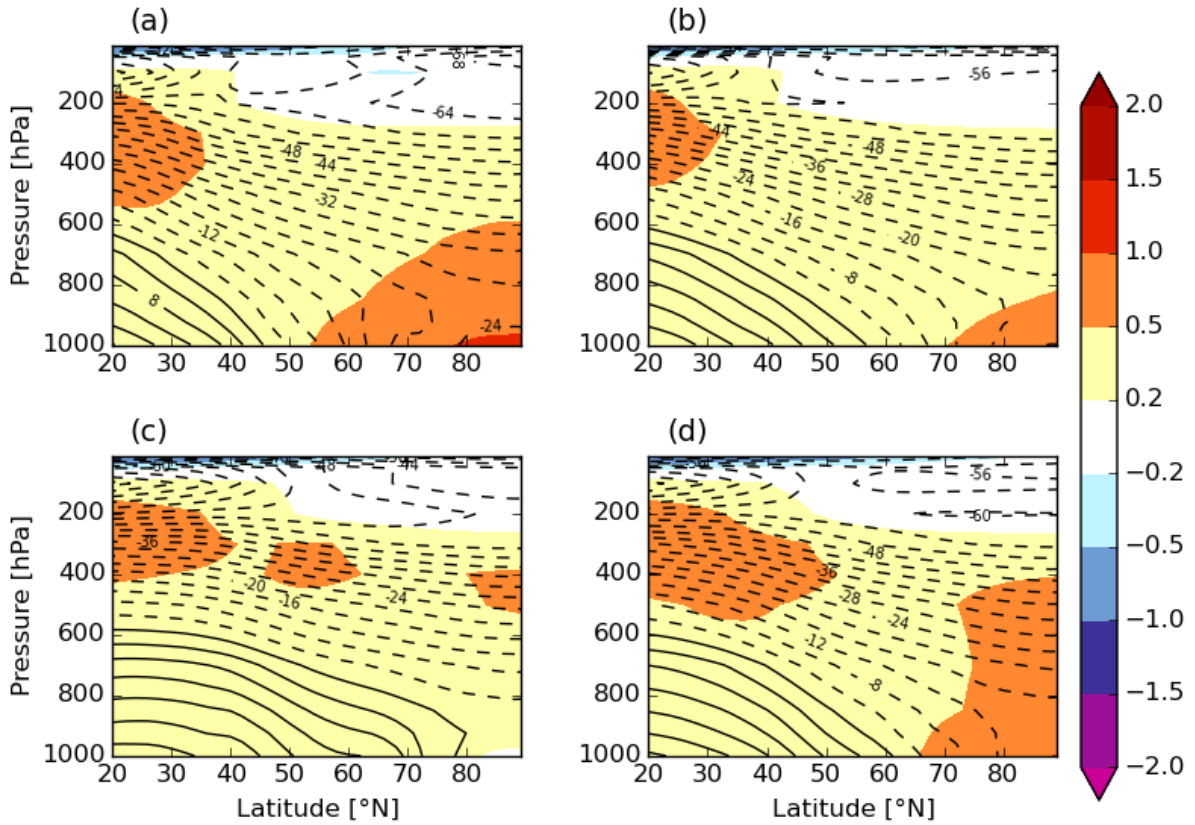
491  
 492  
 493  
 494

Fig. 4: As in Fig. 3 but with 1.65\*CO<sub>2</sub> concentration between 30 and 60°N (in the Northern mid-latitudes).



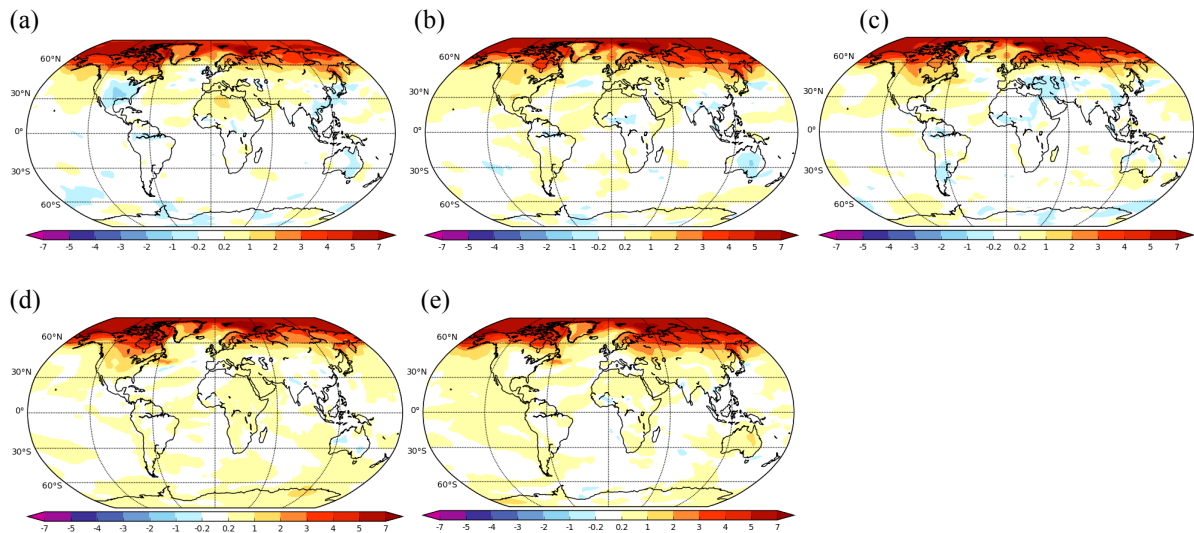
495  
 496  
 497  
 498  
 499  
 500

Fig. 5: As in Fig. 3 but with 4\*CO<sub>2</sub> concentration between 30 and 60°N (in the Northern mid-latitudes) scaled with the difference in forcing areas (area of Arctic divided by area of the Northern mid-latitudes).



501  
502  
503  
504  
505  
506  
507

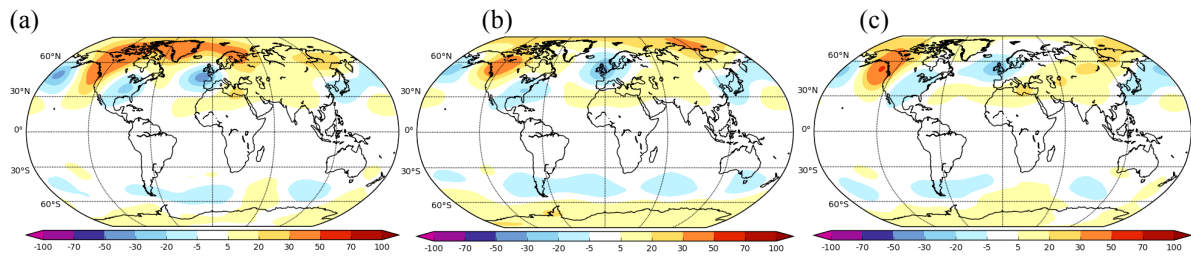
Fig. 6: As in Fig. 3 but with  $4 \times \text{CO}_2$  concentration south of  $60^\circ\text{N}$  (extra-Arctic area) scaled with the difference in forcing areas (area of Arctic divided by area of extra-Arctic).



511  
512  
513  
514  
515  
516  
517  
518  
519  
520  
521

Fig. 7: Response in winter 2 m temperature (K) in 60N simulation, averaged over the first 30 years after regionally quadrupling  $\text{CO}_2$ , (b) averaged over the second 30 years, (c) averaged over the third 30 years, (d) averaged over the fourth 30 years, and (e) averaged over the last 30 years.

522

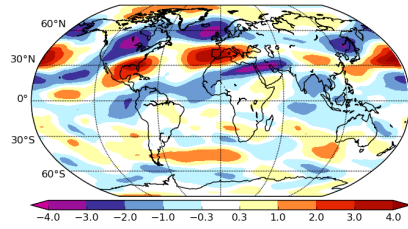


523

524

525 Fig. 8: Response in winter 500 hPa geopotential height (m) in (a) 60N simulation, (b) 70N simulation, and (c)  
526 SICE simulation averaged over the first 30 years after regionally quadrupling CO2.

527



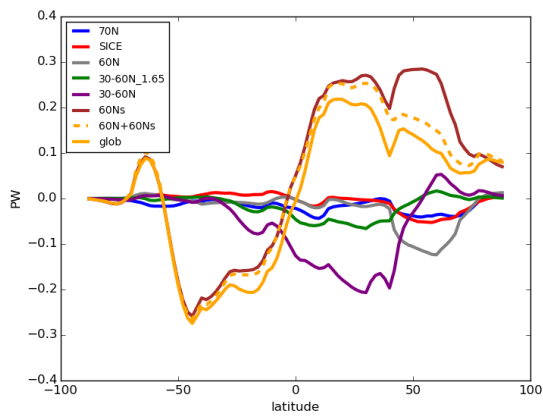
528

529

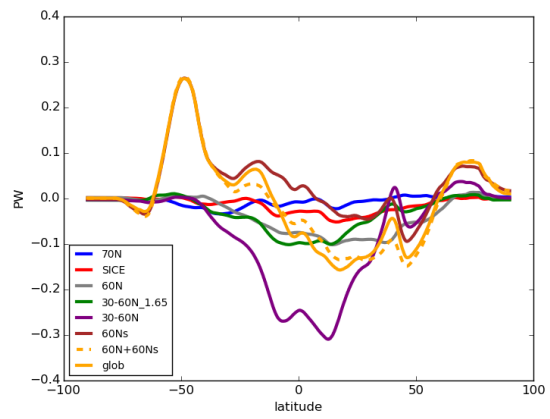
530 Fig. 9: Response in winter 300 hPa u component (m/s) in 60N simulation averaged over the first 30 years after  
531 regionally quadrupling CO2.

532

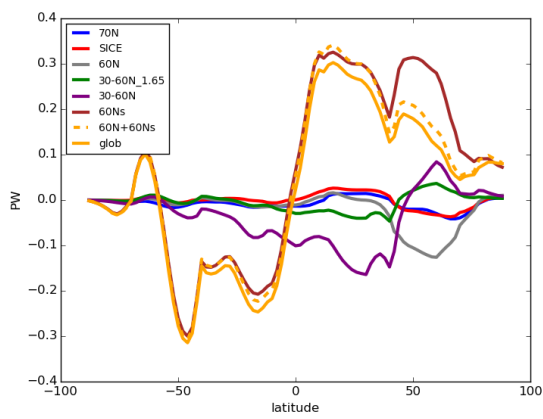
533 (a)



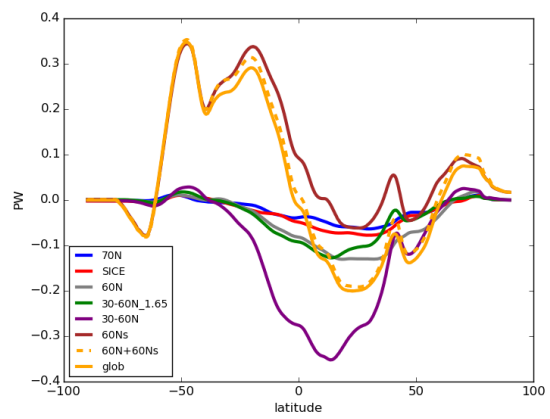
(b)



534  
535 (c)



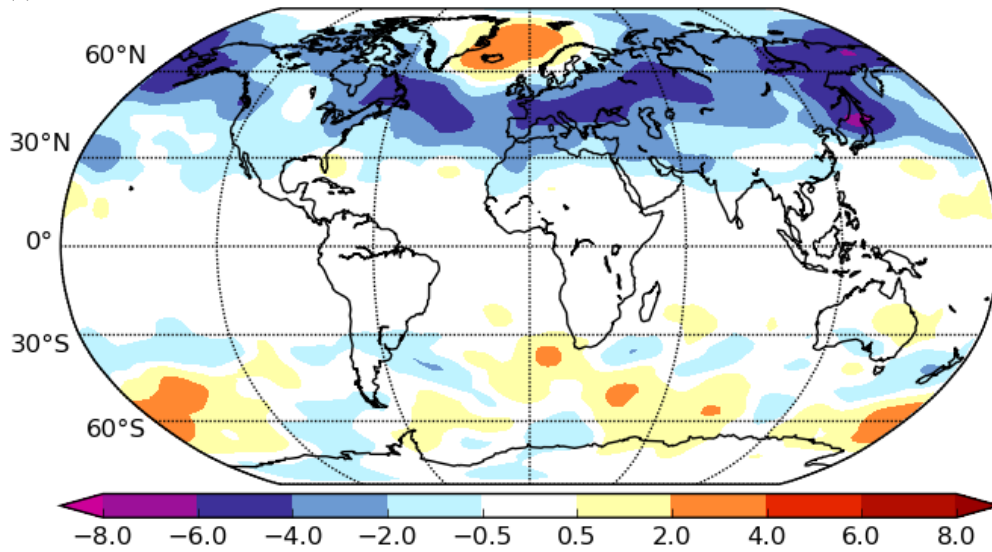
(d)



536  
537  
538  
539  
540  
541  
542

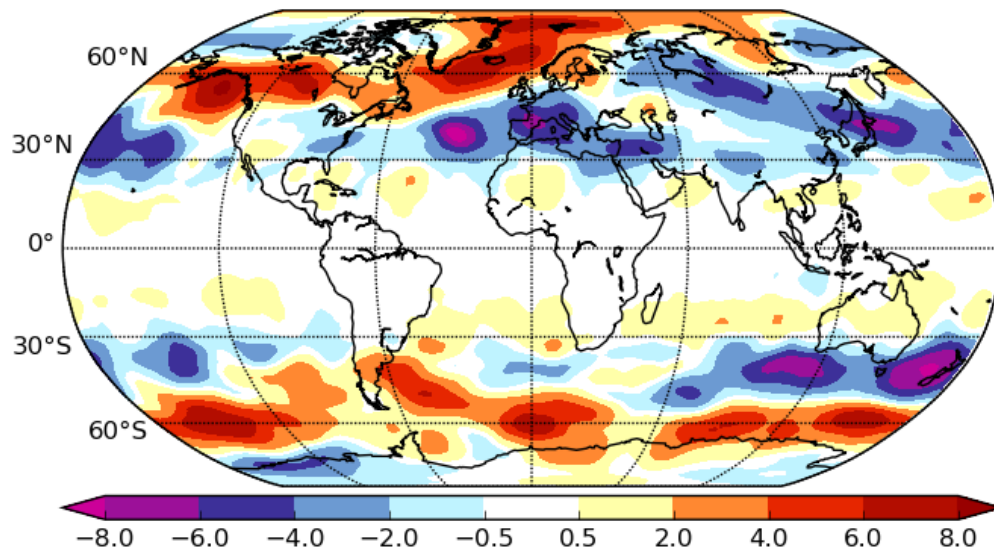
Fig. 10: Northward (a) atmospheric and (b) oceanic energy transport response (PW) averaged over the first 30 years. (c) and (d) as (a) and (b) but for the last 120 years. The orange dashed line shows the sum of the anomalies from the 60N and the 60Ns simulation. The non-zero energy transport at 90°N is due to the uptake of heat from the ocean and indicates that the ocean is not in equilibrium, especially in 60Ns and glob simulations.

(a)



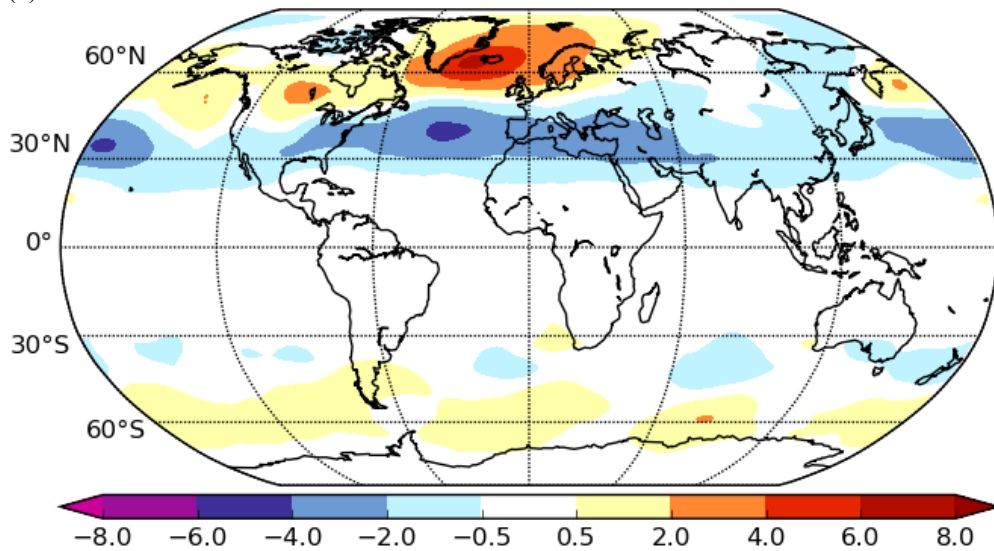
543  
544 (b)





545  
546

(c)



547

548

549

550

551

552

553

554

555

556

557

558

559

560

561

562

563

564

565

566

567

568

569

570

571

572

Fig. 11: Response in synoptic activity in 500 hPa (m) for the last 120 years (a) for 60N, (b) for 30-60N\_1.65, and (c) for 30-60N scaled with the forcing areas.

## References

- Ayarzagüena B, Screen JA (2016) Future Arctic sea ice loss reduces severity of cold air outbreaks in mid-latitudes. *Geophysical Research Letters* 43:2801-2809. <https://doi.org/10.1002/2016GL068092>
- Ayarzagüena B, Polvani LM, Langematz U, Akiyoshi H, Bekki S, Butchart N, Dameris M, Deushi M, Hardiman SC, Jöckel P, Klekociuk A, Marchand M, Michou M, Morgenstern O, O'Connor FM, Oman LD, Plummer DA, Revell L, Rozanov E, Saint-Martin D, Scinocca J, Stenke A, Stone K, Yamashita Y, Yoshida K, Zeng G (2018) No robust evidence of future changes in major stratospheric sudden warmings: a multi-model assessment from CCM1. *Atmospheric Chemistry and Physics* 18:11277-11287. <https://doi.org/10.5194/acp-18-11277-2018>
- Cohen J, Screen JA, Furtado JC, Barlow M, Whittleston D, Coumou D, Francis J, Dethloff K, Entekhabi D, Overland J, Jones J (2014) Recent Arctic amplification and extreme mid-latitude weather. *Nature Geoscience* 7: 627-637. <https://doi.org/10.1038/ngeo2234>
- Cohen J, Zhang X, Francis J, Jung T, Kwok R, Overland J, Taylor PC, Lee S, Laliberte F, Feldstein S, Maslowski W, Henderson G, Stroeve J, Coumou D, Handorf D, Semmler T, Ballinger T, Hell M, Kretschmer M, Vavrus S, Wang M, Wang S, Wu Y, Vihma T, Bhatt U, Ionita M, Linderholm H, Rigor I, Rouston C, Singh D, Wendisch M, Smith D, Screen J, Yoon J, Peings Y, Chen H, Blackport R (2018) Arctic change and possible influence on mid-latitude climate and weather. *US CLIVAR Report 2018-1*, 41pp. <https://doi.org/10.5065/D6TH8KGW>

573  
574 Garfinkel C, Son S-W, Song K, Aquila V, Oman LD (2017) Stratospheric variability contributed to and  
575 sustained the recent hiatus in Eurasian winter warming. *Geophysical Research Letters* 44:374-382.  
576 <https://doi.org/10.1002/2016GL072035>  
577  
578 Gong T, Feldstein S, Lee S (2017) The role of downward infrared radiation in the recent Arctic winter warming  
579 trend. *Journal of Climate* 30:4937-4949. <https://doi.org/10.1175/JCLI-D-16-0180.1>  
580  
581 Gregory JM, Ingram WJ, Palmer MA, Jones GS, Stott PA, Thorpe RB, Lowe JA, Johns TC, Williams KD  
582 (2004) A new method for diagnosing radiative forcing and climate sensitivity. *Geophysical Research Letters*  
583 31:L03205. <https://doi.org/10.1029/2003GL018747>  
584  
585 Haarsma RJ, Roberts MJ, Vidale PL, Senior CA, Bellucci A, Bao Q, Chang P, Corti S, Fuckar NS, Guemas V,  
586 von Hardenberg J, Hazeleger W, Kodama C, Koenigk T, Leung LR, Lu J, Luo J-J, Mao J, Mizielinski MS,  
587 Mizuta R, Nobre P, Satoh M, Scoccimarro E, Semmler T, Small J, von Storch J-S (2016) High Resolution Model  
588 Intercomparison Project (HighResMIP v1.0) for CMIP6. *Geoscientific Model Development* 9:4185-4208.  
589 <https://doi.org/10.5194/gmd-9-4185-2016>  
590  
591 Jaiser R, Dethloff K, Handorf D (2013) Stratospheric response to Arctic sea ice retreat and associated planetary  
592 wave propagation changes. *Tellus A* 65:19375. <https://doi.org/10.3402/tellusa.v65i0.19375>  
593  
594 Kim B-M, Son S-W, Min S-K, Jeong J-H, Kim S-J, Zhang X, Shim T, Yoon J-H (2014) Weakening of the  
595 stratospheric polar vortex by Arctic sea-ice loss. *Nature Communications* 5:4646.  
596 <https://doi.org/10.1038/ncomms5646>  
597  
598 Kug J-S, Jeong J-H, Jang Y-S, Kim B-M, Folland C-K, Min S-K, Son S-W (2015) Two distinct influences of  
599 Arctic warming on cold winters over North America and East Asia. *Nature Geoscience*. [https://doi.org/](https://doi.org/10.1038/NGEO2517)  
600 [10.1038/NGEO2517](https://doi.org/10.1038/NGEO2517)  
601  
602 Luo B, Wu L, Luo D, Dai A, Simmonds I (2018) The winter midlatitude-Arctic interaction: effects of North  
603 Atlantic SST and high-latitude blocking on Arctic sea ice and Eurasian cooling. *Climate Dynamics*.  
604 <https://doi.org/10.1007/s00382-018-4301-5>.  
605  
606 Overland J, Francis JA, Hall R, Hanna E, Kim S-J, Vihma T (2015) The melting Arctic and midlatitude weather  
607 patterns: are they connected? *Journal of Climate*, 28:7917-7932. <https://doi.org/10.1175/JCLI-D-14-00822.1>  
608  
609 Overland JE, Dethloff K, Francis JA, Hall RJ, Hanna E, Kim S-J, Screen JA, Shepherd TG, Vihma T (2016)  
610 Nonlinear response of mid-latitude weather to the changing Arctic. *Nature Climate Change* 6:992–999.  
611 <https://doi.org/10.1038/NCLIMATE3121>  
612  
613 Pedersen RA, Cvijanovic C, Langen PL, Vinther BM (2016) The impact of regional Arctic sea ice loss on  
614 atmospheric circulation and the NAO. *Journal of Climate* 29:889-902. <https://doi.org/10.1175/JCLI-D-15-0315.1>  
615  
616 Petrie RE, Shaffrey LC, Sutton RT (2015) Atmospheric impact of Arctic sea ice loss in a coupled ocean-  
617 atmosphere simulation. *Journal of Climate* 28:9606-9622. <https://doi.org/10.1175/JCLI-D-15-0316.1>  
618  
619 Pithan F, Mauritsen T (2014) Arctic amplification dominated by temperature feedbacks in contemporary climate  
620 models. *Nature Geoscience* 7:181-184. <https://doi.org/10.1038/NGEO2071>  
621  
622 Rackow T, Goessling HF, Jung T, Sidorenko D, Semmler T, Barbi D, Handorf D (2018) Towards multi-  
623 resolution global climate modeling with ECHAM6-FESOM. Part II: climate variability. *Climate Dynamics*  
624 50:2369-2394. <https://doi.org/10.1007/s00382-016-3192-6>  
625  
626 Rackow T, Sein D, Semmler T, Danilov S, Koldunov N, Sidorenko D, Wang Q, Jung T (2019) Sensitivity of  
627 deep ocean biases to horizontal resolution in prototype CMIP6 simulations with AWI-CM 1.0. *Geoscientific*  
628 *Model Development Discussion*. <https://doi.org/10.5194/gmd-2018-192>  
629  
630 Screen JA, Deser C, Smith DM, Zhang X, Blackport R, Kushner PJ, Oudar T, McCusker KE, Sun L (2018)  
631 Consistency and discrepancy in the atmospheric response to Arctic sea-ice loss across climate models. *Nature*  
632 *Geoscience* 11:155-163. <https://doi.org/10.1038/s41561-018-0059-y>  
633

634 Screen JA, Simmonds I, Deser C, Tomas R (2013) The atmospheric response to three decades of observed Arctic  
635 sea ice loss. *Journal of Climate* 26:1230-1248. <https://doi.org/10.1175/JCLI-D-12-00063.1>  
636

637 Semmler T, McGrath R, Wang S (2012) The impact of Arctic sea ice on the Arctic energy budget and on the  
638 climate of the Northern mid-latitudes. *Climate Dynamics* 39:2675-2694. [https://doi.org/10.1007/s00382-012-](https://doi.org/10.1007/s00382-012-1353-9)  
639 1353-9  
640

641 Semmler T, Jung T, Serrar S (2016a) Fast atmospheric response to a sudden thinning of Arctic sea ice. *Climate*  
642 *Dynamics* 46:1015-1025. <https://doi.org/10.1007/s00382-015-2629-7>  
643

644 Semmler T, Stulic L, Jung T, Tilinina N, Campos C, Gulev S, Koracin D (2016b) Seasonal atmospheric  
645 responses to reduced Arctic sea ice in an ensemble of coupled model simulations. *Journal of Climate* 29:5893-  
646 5913. <https://doi.org/10.1175/JCLI-D-15-0586.1>  
647

648 Seviour WJM (2017) Weakening and shift of the Arctic stratospheric polar vortex: internal variability or forced  
649 response? *Geophysical Research Letters* 44:3365-3373. <https://doi.org/10.1002/2017GL073071>  
650

651 Sidorenko D, Rackow T, Jung T, Semmler T, Barbi D, Danilov S, Dethloff K, Dorn W, Fieg K, Goessling HF,  
652 Handorf D, Harig S, Hiller W, Juricke S, Losch M, Schröter J, Sein DV, Wang Q (2015) Towards multi-  
653 resolution global climate modeling with ECHAM6-FESOM. Part I: model formulation and mean climate.  
654 *Climate Dynamics* 44:757-780. <https://doi.org/10.1007/s00382-014-2290-6>  
655

656 Smith DM, Screen JA, Deser C, Cohen J, Fyfe JC, Garcia-Serrano J, Jung T, Kattsov V, Matei D, Msadek R,  
657 Peings Y, Sigmond M, Ukita J, Yoon J-H, Zhang X (2018) The Polar Amplification Model Intercomparison  
658 Project (PAMIP) contribution to CMIP6: investigating the causes and consequences of polar amplification.  
659 *Geoscientific Model Development Discussions*. <https://doi.org/10.5194/gmd-2018-82>  
660

661 Stuecker MF, Bitz CM, Armour KC, Proistosescu C, Kang SM, Xie S-P, Kim D, McGregor S, Zhang W, Zhao  
662 S, Cai W, Dong Y, Jin F-F (2018) Polar amplification dominated by local forcing and feedbacks. *Nature Climate*  
663 *Change*. <https://doi.org/10.1038/s41558-018-0339-y>  
664

665 Sun L, Deser C, Tomas RA (2015) Mechanisms of stratospheric and tropospheric circulation response to  
666 projected Arctic Sea ice loss. *Journal of Climate* 28:7824-7845. <https://doi.org/10.1175/JCLI-D-15-0169.1>  
667

668 Tamarin T, Kaspi Y (2017) The poleward shift of storm tracks under global warming: A Lagrangian perspective.  
669 *Geophysical Research Letters*. <https://doi.org/10.1002/2017GL073633>  
670

671 Vavrus SJ (2018) The influence of Arctic Amplification on Mid-latitude Weather and Climate. *Current Climate*  
672 *Change Reports* 4:238-249. <https://doi.org/10.1007/s40641-018-0105-2>  
673

674 Woods C, Caballero R (2016) The role of moist intrusions in winter Arctic warming and sea ice decline. *Journal*  
675 *of Climate* 29:4473-4485. <https://doi.org/10.1175/JCLI-D-15-0773.1>  
676

677 Zappa G, Pithan F, Shepherd G (2018) Multimodel evidence for an atmospheric circulation response to Arctic  
678 sea ice loss in the CMIP5 future projections. *Geophysical Research Letters*, 45:1011-1019.  
679 <https://doi.org/10.1002/2017GL076096>